Vol 17 No 6, June 2008
1674-1056/2008/17(06)/2184-07

Chinese Physics B

© 2008 Chin. Phys. Soc.
and IOP Publishing Ltd

Synthesis and characterization of axially periodic Zn_2SnO_4 dendritic nanostructures*

Shen Jun(沈 俊)[a)b)], Ge Bing-Hui(葛炳辉)[a)b)], Chu Wei-Guo(褚卫国)[c)],
Luo Shu-Dong(罗述东)[a)b)], Zhang Zeng-Xing(张增星)[a)b)], Liu Dong-Fang(刘东方)[a)b)],
Liu Li-Feng(刘利峰)[a)b)], Ma Wen-Jun(马文君)[a)b)], Ren Yan(任 彦)[a)b)],
Xiang Yan-Juan(向彦娟)[a)b)], Wang Chao-Ying(王超英)[a)],
Wang Gang(王 刚)[a)], and Zhou Wei-Ya(周维亚)[a)†]

[a)] *Beijing National Laboratory for Condensed Matter Physics, Institute of Physics, Chinese Academy of Sciences, Beijing* 100190, *China*
[b)] *Graduate School of the Chinese Academy of Sciences, Beijing* 100039, *China*
[c)] *National Center for Nanoscience and Nanotechnology, Beijing* 100190, *China*

(Received 4 December 2007; revised manuscript received 4 January 2008)

Zn_2SnO_4 (ZTO) nanowires with a unique dendritic nanostructure were synthesized via a simple one-step thermal evaporation and condensation process. The morphology and microstructure of the ZTO nanodendrite have been investigated by means of field emission scanning electron microscopy (SEM), x-ray diffraction (XRD) and high-resolution transmission electron microscopy (HRTEM). SEM observation revealed the formation of branched nanostructures and showed that each branch exhibited a unique periodic structure formed by a row of overlaid rhombohedra of ZTO nanocrystals along the axis of the nanobranch. HRTEM studies displayed that the branches grew homoepitaxially as single-crystalline nanowires from the ZTO nanowire backbone. A possible growth model of the branched ZTO nanowires is discussed. To successfully prepare branched structures would provide an opportunity for both fundamental research and practical applications, such as three-dimensional nanoelectronics, and opto-electronic nanodevices.

Keywords: Zn_2SnO_4, epitaxial growth, dendrite, photoluminescence
PACC: 6146, 8110B, 8160C, 7865

1. Introduction

Nanostructures, such as nanowires and nanobelts, are well-known as key building blocks for nanoscale science and technology. It is necessary to implement the 'bottom-up' approach in nanoscale fabrication so that specific nanostructures with unique physical properties could be assembled into photonic and electronic devices. Semiconductor nanowires are promising low-dimensional materials with a wide range of photonic and electronic applications, including field-effect transistors,[1] lasers,[2] photodetectors[3] and sensors,[4] etc. Diverse applications are enabled by synthetic control over nanowire composition and geometry. Branched and/or hierarchical nanostructures not only increase the complexity of nanowire materials but also offer the flexible building blocks, which will yield diverse functions based on well-defined sequence/structure variations. Recently, a few groups have synthesized branched and multi-branched hierarchical nanowire structures. Wan *et al*[5] have grown ITO nanowire arrays by the vapour transport method based on the vapour–liquid–solid (VLS) growth mode at 800–900°C, using indium and tin monoxide powders as the source materials. Samuelson *et al*[6] have synthesized GaP nanotrees with the assistance of Au aerogel through multi-step vapour processes. In Ref.[7–10], it has been systematically investigated that the hierarchical ZnO and In_2O_3 nanostructures grown by chemical vapour deposition process, and the orientation relationship was analysed between the core and the branches.

Zn_2SnO_4 (ZTO, E_g=3.6 eV) is one of the significant functional materials with high electrical conductivity and low absorption of visible light, which make it a good candidate for wide applications, including sensors and photovoltaic elements.[11−13] To date, many efforts have been made to fabricate ZTO nanos-

*Project supported by the National Natural Science Foundation of China (Grant Nos 10334060 and 90406022) and the National Basic Research Program of China (Grant No 2005CB623602).
†Correspondence author. E-mail: wyzhou@aphy.iphy.ac.cn

tructures by the 'bottom-up' approach, such as wires, belts, and rings etc.[14−18] The ZTO dendrite-shaped nanostructures could be a new candidate for nanodevices. Meanwhile, the investigation of the crystallographic relation between branches and trunks can help us to understand the growth process in detail. In this paper, we report that a unique nanoscale ZTO dendritic structure could be realized by a simple one-step thermal evaporation and condensation process. A possible mechanism of the formation of dendrite-shaped structures is discussed. The nanodendrite structures might have potential applications in optical and optoelectronic devices.

2. Experimental details

ZTO nanowires were grown in a horizontal tubular furnace. The source material was a mixture of commercial ZnO powder, SnO powder and activated carbon powder (weight ratio 6:4:1). The silicon (Si) slices coated with gold film of 0.5–1.0 nm in thickness were used as the substrates. After the furnace was heated up to the desired temperature of 900°C, the source and the Si substrates, held in a slightly smaller quartz tube, were loaded into the furnace quickly in a place to keep the source at the centre of the furnace tube while the Si substrates at the downstream site 12–15 cm away from the source. Then the furnace tube was evacuated by a mechanical pump and aerated with Ar gas and a little O_2. During the growth, the furnace was maintained at 900°C and the pressure in the reaction tube was kept at about 2 Pa at a gas flow rate of 300 sccm (standard cubic centimetres per minute) Ar and 1 sccm O_2. The reaction time was about 3 h. Then the products were quenched to room temperature.

A thick layer of white fluffy product was collected on the Si substrates after the reaction. The morphology and the structure of the products were characterized by x-ray powder diffraction (XRD, PANalytical X'Pert PRO) with Cu-K_α radiation (λ=0.15406 nm), field-emission scanning electron microscopy (SEM, Hitachi S-5200) equipped with energy disperse x-ray (EDX) spectrometer (Thermoelectron), and high-resolution transmission electron microscope (HRTEM, Philips CM200ST/FEG and FEI Tecnai G^2, accelerating voltage 200 kV) with electron diffraction. The room temperature photoluminescence (PL) spectrum was recorded in the spectral range of 350–800 nm using a He–Cd laser (325.0 nm) as the excitation light source.

3. Results and discussion

A typical XRD pattern of the as-deposited product is shown in Fig.1. Most peaks can be indexed in the face-centred cubic spinel structure of ZTO with lattice constant of a=0.8650 nm, which is consistent with the standard data file (PDF No. 24–1470). The residual weak peaks can be indexed as ZnO (PDF No. 36–1451), indicating that there are small quantities of ZnO in the as-prepared product. Most of reported results about ZTO nanostructures also showed the existence of a little ZnO impurity.[14−18]

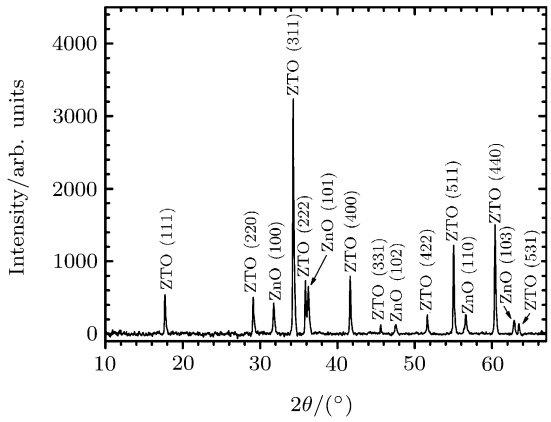


Fig.1. XRD pattern of the as-synthesized product.

Representative SEM images of the as-synthesized products on Si substrates are shown in Fig.2. The low-magnification SEM image reveals that the products mostly consist of dendritic nanostructures and a portion of nanowires can be of over several hundreds of micrometres in length (as shown in Fig.2(a)). On one dendrite, the branch arrays are distributed only on one side of a rough trunk to form a dendritic structure as shown in Fig.2(b), implying that the branches have a preferred growth direction and possess a well-defined relationship with the trunk.[19] Moreover, the branches have a nearly uniform diameter about 75 nm, distributed as a pseudo-periodic array, and connected to the trunk through a pyramid. The high-magnification image in Fig.2(c) reveals that the branch has its own periodic structure formed by a row of overlaid rhombohedra of nanocrystals along the axis of the branch, and there are a number of periodic stripes on the branch. Similar stripes were also found on the trunk. The image clearly illustrates the

pyramid at each junction between the trunk and the branch. Besides the ZTO dendrites, there are some axially periodic ZTO nanowires as shown in Fig.2(d), which are similar to the morphology of the branch and the trunk.

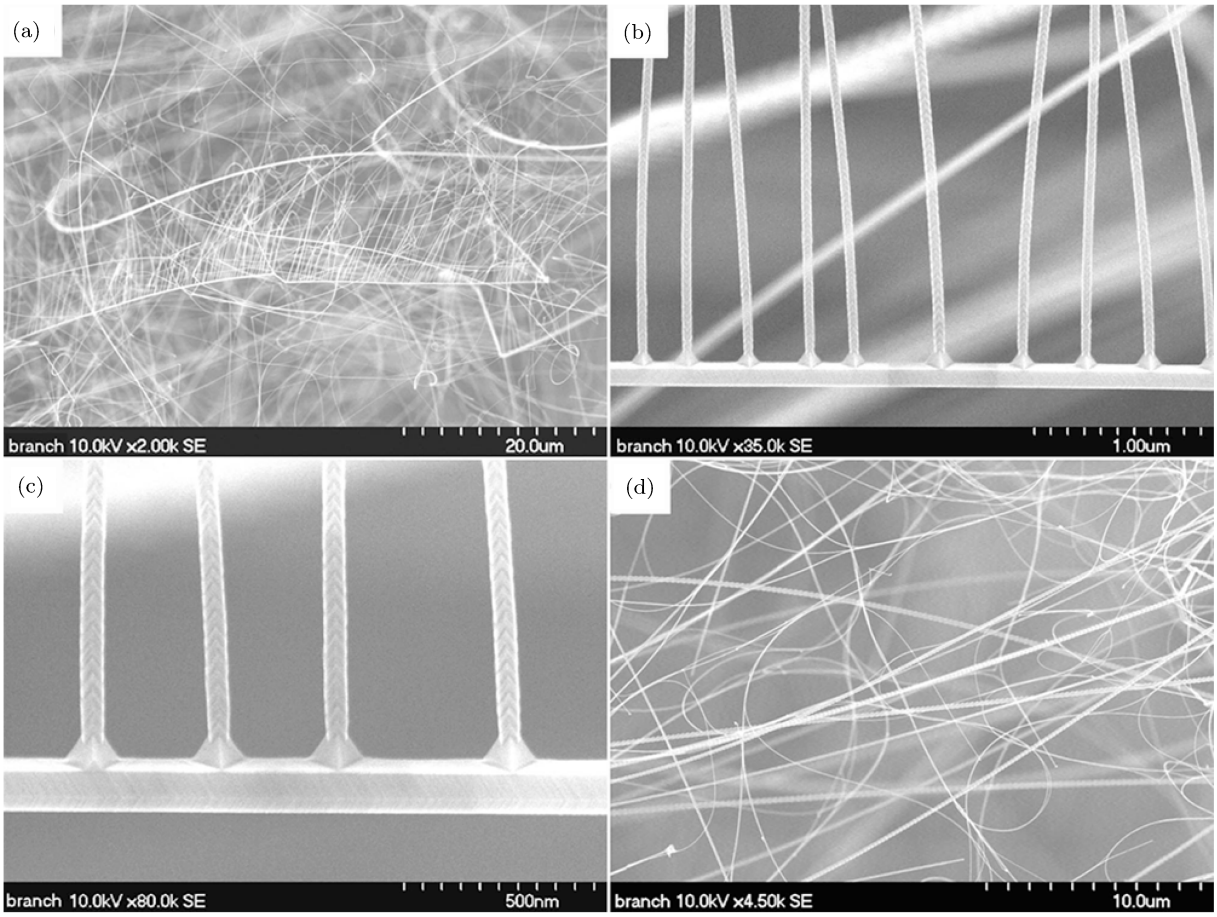


Fig.2. Representative SEM images of the ZTO nanostructures: (a) Low-magnification image of the dendritic ZTO nanostructures. (b) Image showing the branches grown exclusively on one side of and perpendicular to the trunk. (c) High-magnification image of an axially periodic ZTO nanobranch structure. (d) SEM image of ZTO nanowires.

To obtain more detailed information about the structure and composition of our product, the structure and the morphology of the ZTO dendrite were further characterized by TEM and EDX. The as-synthesized products were transferred into the ethanol solution and dispersed onto a copper grid with porous carbon film. Figure 3(a) is a bright-field TEM image of one of the dendritic structures, which shows that the branch with a diameter of about 75 nm grows epitaxially from the trunk, and a pyramidal pedestal exists at the junction between the branch and trunk. The typical EDX spectra obtained from the branch and trunk are presented respectively in the upper right and lower left insets in Fig.3(a). The EDX spectra reveal that both the branch and the trunk consist of Zn, Sn and O elements only (Cu line comes from the copper grid). Furthermore, HRTEM is employed to analyse the trunk, branch and junction. The HRTEM image in Fig.3(b) is taken from the trunk, which demonstrates that the trunk basically keeps well crystallized with a clear lattice fringe, and the interplanar spacing is 0.296 nm, corresponding to that of ZTO (220) planes. The inset is the fast Fourier transform (FFT) of the corresponding HRTEM image, indicating that the growth orientation of the trunk can be assigned to [110]. Figure 3(c) is a typical HRTEM image of the branch, and the inset is the typical selected area electron diffraction (SAED) pattern. The clear lattice

fringes in the HRTEM image confirm the high crystalline nature of the branch with few defects. The growth orientation of the as-synthesized axially periodic branch can be indexed as $[1\bar{1}1]$ according to the SAED pattern. Also shown in the HRTEM image in Fig.3(c), the lattice spacing is about 0.494 nm, corresponding to the spacing of the (111) planes of ZTO spinel structure. Figure 3(d) is a typical HRTEM image of pyramidal junction corresponding to the dashed circle region in Fig.3(a), which reveals that no defects are observed at the junction, and the fringes are continuous in the region of junction, confirming that the dendritic nanowire extending from the pyramidal base has a uniform structure and grows epitaxially from the trunk. All of the above mentioned results demonstrate that the branch grows from the $(1\bar{1}1)$ plane of the ZTO trunk, which explains the perpendicular growth of the branch with respect to the growth orientation of the trunk. Moreover, the coherent growth of ZTO {111} surfaces induces periodic microfaceting in every branch and the zigzag appearance.

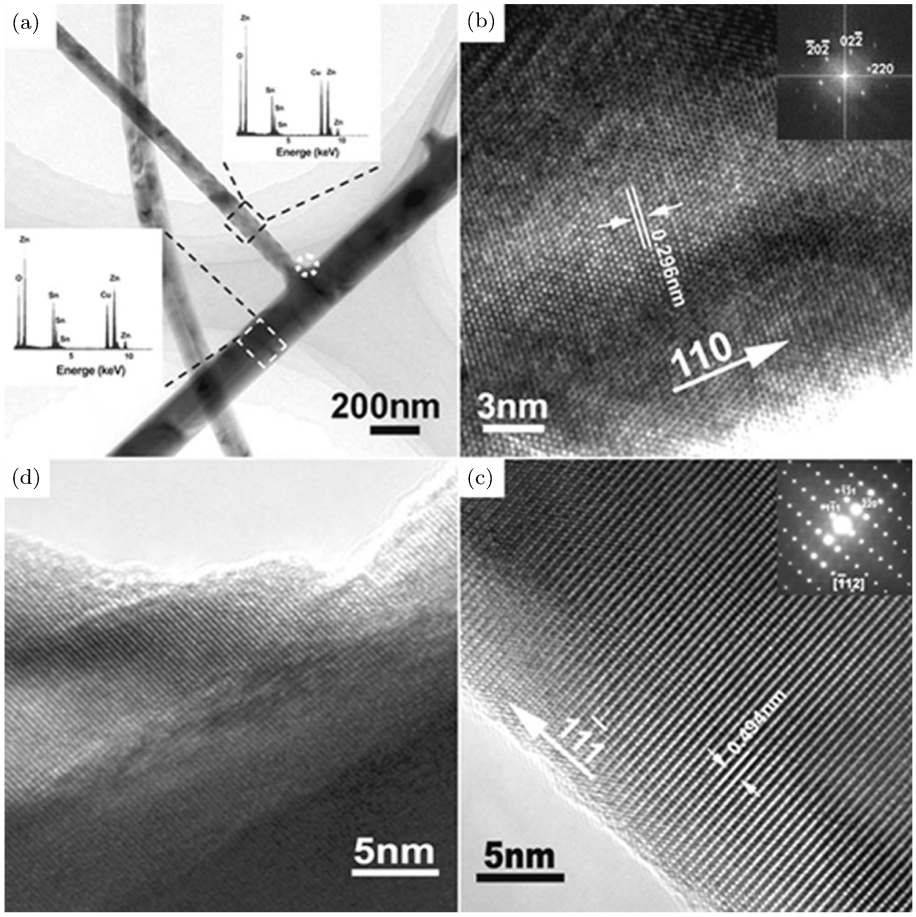


Fig.3. (a) Bright-field TEM image of one of the dendritic structures. The upper right and lower left insets corresponding to the typical EDX spectra of the branch and trunk, respectively. (The dashed circle shows the region enlarged in the HRTEM image.) (b) HRTEM image of the trunk. (c) HRTEM image showing the perfect and identical crystal structure of one branch on ZTO dendritic structure. (d) Corresponding HRTEM image of the dendrite junction.

In addition, a few twinning structures can be observed in some branches of a ZTO dendrite. Figures 4(a)–4(c) shows the bright TEM image of one branch with twinning structures and the corresponding diffraction pattern. The white arrow head in Fig.4(a) indicates the clear twinning boundary. Figure 4(b) presents the HRTEM image showing the morphologic property of twinning boundary. It is known that

the (111) twinned crystals have a relative rotational angle of 70.5°. Therefore, the inner angle of the zigzag as indicated by the white lines is about 141°, in good agreement with the theoretical and experimental results.[20] The electron diffraction pattern shown in Fig.4(c) arises definitely from the (111) twinning structure commonly appearing in the fcc systems. All diffraction spots in the present pattern can be indexed by using twinned nanocrystals, which also proves that the periodic microfacets in every branch are the ZTO (111) facets.

The growth process can be understood via the investigation of the details of growth. Fig.5(a) is a typical image of ZTO nanodendrite with the end of the trunk (a-1 the high-magnification image of the trunk tip), which shows the Au-rich nanoparticle at the tip of the trunk. Also, every branch has a tip with one Au-rich particle for the short-time experimental sample shown in Figs.5(b) and (b-1), which further reveal the growth of the branch. The lowest two EDX spectra in Fig.5 correspond to the images of the tip particles in Figs.(a-1) and (b-1), respectively.

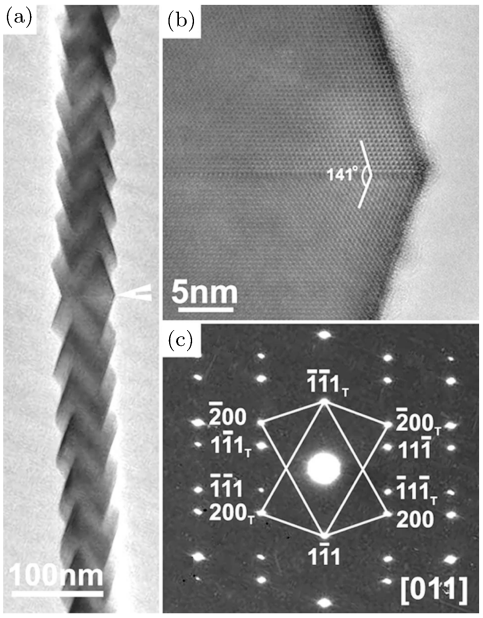


Fig.4. (a) TEM image of a ZTO nanobranch with twinning structures. A twinning structure is shown by an arrow head. (b) HRTEM image of a local part of the ZTO nanobranch, showing the twinning boundary clearly. (c) Corresponding electron diffraction pattern of the twinning structure.

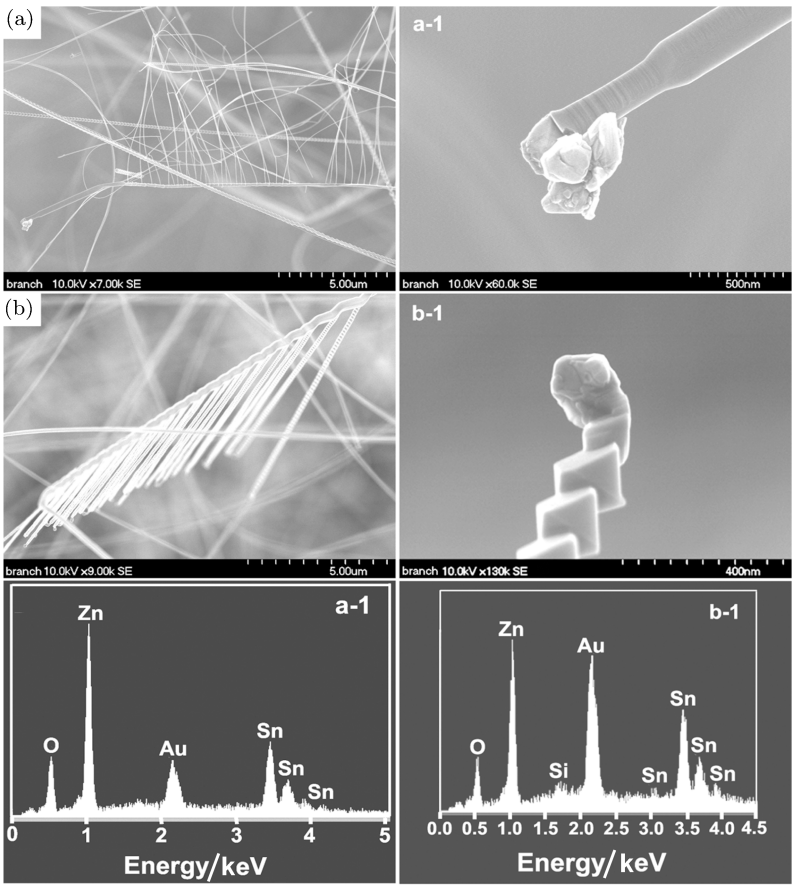


Fig.5. (a) The SEM image of ZTO nanodendrite with the end of the trunk ((a-1) the high-magnification image of the trunk tip). (b) A typical image of ZTO dendrite with one particle on the tip of every branch ((b-1) is a typical tip of a branch with one particle). The lowest two EDX spectra correspond to the particles in (a-1) and (b-1) images respectively.

As discussed above, the ZTO dendritic growth process is mainly a VLS one,[21] including the Au-assistant catalytic reaction for the trunk and the branch. Here, we propose the catalyst-assisted epitaxy as the growth mechanism of the dendritic structure in the VLS growth process. The process includes the following typical steps:

Firstly, zinc and tin vapour, obtained by a carbothermal reduction process of ZnO and SnO, react with Au film to form Au-Zn-Sn alloy. Then this alloy further reacts with oxygen, and the nanowires of ZTO nucleate after the alloy becomes supersaturated with reactant species and grow out, as shown in Fig.6(a).[22] Secondly, The nanowires grown at the first stage can serve as a substrate for the secondary deposition of the Au catalyst to grow branches (Fig.6(b)). Thirdly, every particle on a ZTO nanowire trunk then serves as a preferential site for absorbing the reactant species (Zn, Sn and O species). In the absorption process, the particle will be a little bigger until the supersaturation (Fig.6(c)). A key issue is the formation of pyramidal mounds on the nanowire trunk during growth while the reactant vapour is available (Fig.6(d)). Once the catalyst particle is supersaturated, a nucleus will be formed and further grow up with a certain crystallographic relation. In our experiments, pyramidal mounds have been found on the nanowire substrate during its growth, indicating that the growth is roughly a three-dimensional overlayer. The time evolution of this type of junction may result from two possible effects: a noisy (thermal) flux of impinging atoms and the relaxation of the structure. The latter governs the rearrangement of different atoms once they arrive at the surface, because the different crystal face has the different growth kinetic energy. Consequently, it is essential to consider the specific relaxation mechanism that is relevant to the growth on crystalline surfaces: nucleation, surface diffusion, and diffusion over the crystalline surface step ledges, which needs further investigation. Finally, the axial periodic nanobranches grow parallel to each other and perpendicular to the axial direction of the trunk (Fig.6(e)). Thus, epitaxial growth can occur at the nucleation stage of branch growth, and the branches may reproduce the structure of the backbone substrate; this fact can interpret the result that no defects have been found at the junction.

PL measurements of the as-synthesized sample were carried out at room temperature at an exciton wavelength being 325 nm. The PL signals were collected on ensemble product with both nanodendrites

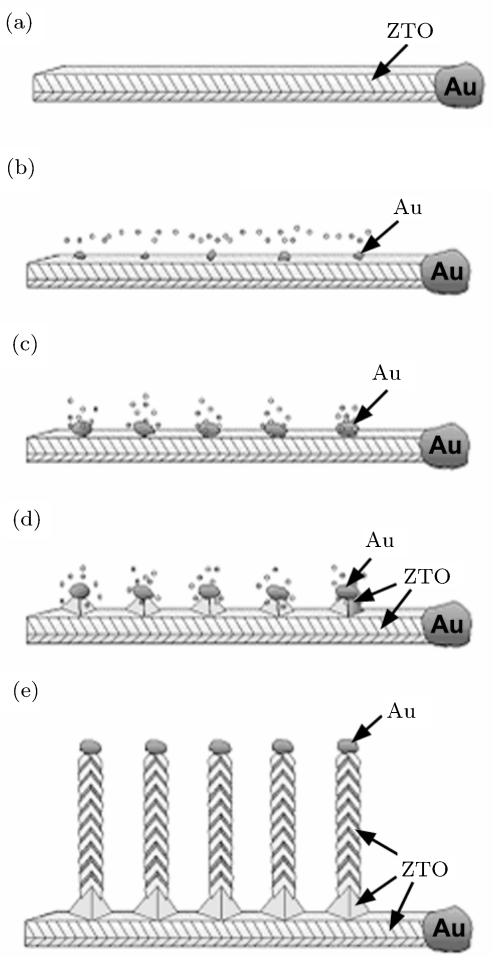


Fig.6. Schematic diagram of the growth mechanism of ZTO nanodendrite. (a) A nucleation and growth process for the substrate nanowire occurs by Au catalysis. (b) The deposition of tin and zinc species on the nanowire surface with the assistance of Au particles. (c) Growth of the Au particles with the absorption. (d) Formation of pyramidal base on the nanowire substrate. (e) Growth of the axially periodic nanobranches.

and nanowires. Thus the PL result obtained should reflect an average characteristic of the sample. The PL spectra taken for different sites show similar feature, that is to say the sample is uniform. Figure 7 illustrates the dominant emission peaks located in violet, blue, and orange regions. A multi-peak Lorentzian fit gives three Lorentzian bands centering at 380, 438, and 598 nm, respectively. As indicated in Fig.7, the Lorentzian curve fits well to the experimental one, which demonstrates that the PL spectrum mainly consists of three emission bands at 380, 438 and 598 nm. Due to the presence of ZnO in our samples as shown in the XRD pattern, the emission band centred at 380 nm could be accounted to the ZnO impurity. The two latter emission bands are obviously different from the reported PL spectra of ZTO nanowires that have been assigned to the effects of the oxygen vacancies.[15]

According to the analyses of structure and composition by TEM and EDX, the emission band centred at 438 nm (reported in Ref.[23]) and the seriously broadened orange emission band,which has never been reported elsewhere, should be ascribed to other luminescence centres, such as crystal stoichiometric vacancies or interstitial impurities in the ZTO dendritic structures.

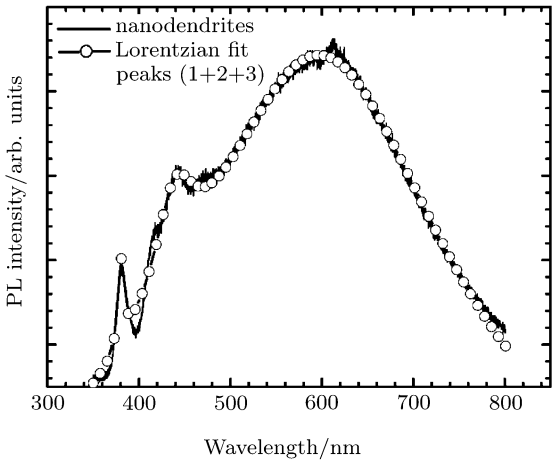


Fig.7. Room-temperature PL spectrum of the as-synthesized sample.

4. Conclusions

ZTO dendritic nanowires have been successfully synthesized by evaporating a powder mixture of ZnO, SnO and activated carbon. The morphology and the structure of the unique type of ZTO dendrites have been characterized in detail by SEM, HRTEM, SAED and EDX. The growth mechanism is proposed for interpreting the formation of the dendritic structure. Moreover, the room temperature PL spectrum shows that it mainly includes three parts: the violet emission band centering at about 380 nm, the blue emission band centering at about 438 nm and the orange emission band broadened seriously around 598 nm. The hierarchical structures of nanomaterials offer a route for increasing structural complexity and for achieving novel properties of materials.

Acknowledgments

We thank Jiang Zhongwei and Chen Jingran for their technical assistance in PL and XRD measurements.

References

[1] Duan X F, Huang Y, Cui Y, Wang J and Lieber C M 2001 *Nature* **409** 66
[2] Huang M H, Mao S, Feick H, Yan H Q, Wu Y Y, Kind H, Weber E, Russo R and Yang P D 2001 *Science* **292** 1897
[3] Hsu C L, Chang S J, Lin Y R, Li P C, Lin T S, Tsai S Y, Lu T H and Chen I C 2005 *Chem. Phys. Lett.* **416** 75
[4] Ponzoni A, Comini E, Sberveglieri G, Zhou J, Deng S Z, Xu N S, Ding Y and Wang Z L 2006 *Appl. Phys. Lett.* **88** 203101
[5] Wan Q, Wei M, Zhi D, MacManus-Driscoll J L and Blamire M G 2006 *Adv. Mater.* **18** 234
[6] Dick K A, Deppert K, Larsson M W, Martensson T, Seifert W, Wallenberg L R and Samuelson L 2004 *Nat. Mater.* **3** 380
[7] Lao J Y, Huang J Y, Wang D Z and Ren Z F 2003 *Nano Lett.* **3** 235
[8] Wen J G, Lao J Y, Wang D Z, Kyaw T M, Foo Y L and Ren Z F 2003 *Chem. Phys. Lett.* **372** 717
[9] Gao P X and Wang Z L 2004 *Appl. Phys. Lett.* **84** 2883
[10] Wang D L and Lieber C M 2003 *Nat. Mater.* **2** 355
[11] Ko J H, Kim I H, Kim D, Lee K S, Lee T S, Jeong J H, Cheong B, Baik Y J and Kim W M 2006 *Thin Solid Films* **494** 42
[12] Jackson W B, Hoffman R L and Herman G S 2005 *Appl. Phys. Lett.* **87** 193503
[13] Yu J H and Choi G M 2001 *Sensors Actuators* B **72** 141
[14] Wang L S, Zhang X Z, Liao X and Yang W G 2005 *Nanotechnology* **16** 2928
[15] Wang J X, Xie S S, Gao Y, Yan X Q, Liu D F, Yuan H J, Zhou Z P, Song L, Liu L F, Zhou W Y and Wang G 2004 *J. Cryst. Growth* **267** 177
[16] Wang J X, Xie S S, Yuan H J, Yan X Q, Liu D F, Gao Y, Zhou Z P, Song L, Liu L F, Zhao X W, Dou X Y, Zhou W Y and Wang G 2004 *Solid State Commun.* **131** 435
[17] Jie J S, Wang G Z, Han X H, Fang J P, Yu Q X, Liao Y, Xu B, Wang Q T and Hou J G 2004 *J. Phys. Chem.* B **108** 8249
[18] Li Y and Ma X L 2005 *Phys. Status Solidi* A **202** 435
[19] May S J, Zheng J G, Wessels B W and Lauhon L J 2005 *Adv. Mater.* 17 598
[20] Chen H Y, Wang J X, Yu H C, Yang H X, Xie S S and Li J Q 2005 *J. Phys. Chem.* B **109** 2573
[21] Wagner R S and Ellis W C 1964 *Appl. Phys. Lett.* **4** 89
[22] Hu J T, Odom T W and Lieber C M 1999 *Acc. Chem. Res.* **32** 435
[23] Li Z R, Li X L, Zhang X X and Qian Y T 2006 *J. Cryst. Growth* **291** 258